Inorg. Chem. **2009**, *48*, 3840−3847

Is 2.07 Å a Record for the Shortest Pt−S Distance? Revision of Two Reported X-ray Structures

Andrea Ienco, Maria Caporali, Fabrizio Zanobini, and Carlo Mealli*

Istituto di Chimica dei Composti Organometallici, ICCOM-CNR, Via Madonna del Piano 10, Sesto Fiorentino (Firenze) 50019, Italy

Received December 15, 2008

The comparison of the very similar compounds $(Ph_3P)_2Pt(\mu\text{-}S)_2Pt(PPh_3)_2$ (**1**) and $(Ph_2PyP)_2Pt(\mu\text{-}S)_2Pt(PPh_2Py)_2$ (**2**) raises intriguing questions about the reliability of the reported Pt_2S_2 core in **1**, where the Pt−S bonds are the shortest ever reported. Also, the *trans*-annular S···S separation of 2.69 Å is surprisingly shorter in **1** than in **2** (3.01 Å), but no incipient coupling between two S^{2-} bridges seems reasonable in this case. Various considerations lead to reformulate **1** as $[(Ph_3P)_2Pt(\mu\text{-}OH)_2Pt(PPh_3)_2](BF_4)_2$, **3**. The sets of cell parameters for **1** and **3** are not equal but two axes match, and the volume of **1** is exactly double. Simple matrices may be constructed to interconvert the direct and reciprocal crystalline cells, thus corroborating their identity of the compounds. It is concluded that, in the structure solution of **1**, some atoms were either neglected (BF_4^- counterions) or ill identified (sulfido in place of hydroxo bridges), while the structure of **3** was solved by collecting only one-half of the possible reflections (hence, also the different space groups). A new preparation, crystallization and X-ray structure of **3** confirms the above points and dismisses any other theoretical conjecture about two electronically different Pt_2S_2 cores in **1** and **2**.

Introduction

Half S−S bonds between two disulfido ligands at large separations (2.7−2.9 Å) were highlighted in the products of the 2e$^-$ oxidation of the dinuclear compounds $Cp^*M(\mu\text{-}CH_2)_2(\mu\text{-}S_2)MCp^*$ (M = Rh, Ir).[1] In fact, the tetranuclear derivative $[\{Cp^*_2M_2(\mu\text{-}CH_2)_2\}_2](\mu\text{-}S_4)]^{2+}$ contains an elongated S_4^{2-} rectangle formed from the original S_2^{2-} units (Scheme 1). The two single and two half S−S bonds, either parallel (Ir) or orthogonal (Rh) to the M−M linkages, have been supported by theoretical arguments,[2] and the unusual S_4^{2-} ring now starts to be recognized also for new compounds.[3] Moreover, from a search in the Cambridge database (CCDC)[4] it was inferred[2a] that occasionally two parallel S_2^{2-} bridges between two metals, considered separated,[5,6] are instead coupled together. Some experimental evidence of this[7] has also been reported for the complex $[(OTf_2L_2Cu)_2(\mu\text{-}S_4)]$ (L_2 = uncharged dinitrogen chelate).[6] In this case, there must be an inner redox process depending on the nature of the copper metals, which dislike the higher oxidation state +3 (to be associated to the separated disulfido bridges).[2a] Under similar circumstances, more electropositive metals (e.g., Ru or Mn) maintain the opened M_2S_4 ring.[8]

Scheme 1

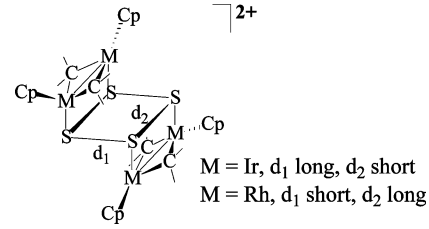

* To whom correspondence should be addressed. E-mail: carlo.mealli@iccom.cnr.it.

(1) (a) Isobe, K.; Ozawa, Y.; Vazquez de Miguel, A.; Zhu, T. W.; Zhao, K. M.; Nishioka, T.; Ogura, T.; Kitagawa, T. *Angew. Chem., Int. Ed. Engl.* **1994**, *33*, 1882. (b) Nishioka, T.; Kitayama, H.; Breedlove, B. K.; Shiomi, K.; Kinoshita, I.; Isobe, K. *Inorg. Chem.* **2004**, *43*, 5688.

(2) (a) Mealli, C.; Ienco, A.; Poduska, A.; Hoffman, R. *Angew. Chem., Int. Ed.* **2008**, *47*, 1. (b) Poduska, A.; Hoffmann, R.; Ienco, A.; Mealli, C. *Chem.—Asian J.* **2008**, *4*, 302–313.

(3) Shenglai, Y.; Milsmann, C.; Bill, E.; Wieghardt, K.; Driess, M. *J. Am. Chem. Soc.* **2008**, *130*, 13536.

(4) (a) Cambridge Structural Database System, Cambridge Crystallographic data Centre, 12 Union Road, Cambridge, CB2 1EZ, U.K. (updated March, 2008). (b) Allen, F. H. *Acta Crystallogr., Sect. B* **2002**, *58*, 380.

(5) Brunner, H.; Merz, A.; Pfauntsch, J.; Serhadli, O.; Wachter, J.; Ziegler, M. L. *Inorg. Chem.* **1988**, *27*, 2055.

(6) York, J. T.; Brown, E. C.; Tolman, W. B. *Angew. Chem., Int. Ed.* **2005**, *44*, 7745.

(7) Sarangi, R.; York, J. T.; Helton, M. E.; Fujisawa, K.; Karlin, K. D.; Tolman, W. B.; Hodgson, K. O.; Hedman, B.; Solomon, E. I. *J. Am. Chem. Soc.* **2008**, *130*, 676.

(8) Mealli, C.; Ienco, A.; Messaoudi, A.; Poduska, A.; Hoffmann, R. *Inorg. Chim. Acta* **2008**, *361*, 3631, and references therein.

10.1021/ic8023748 CCC: $40.75
Published on Web 03/16/2009

Scheme 2

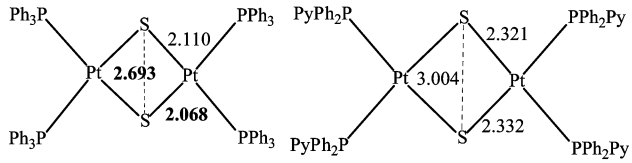

1 **2**

Next, we thought that also the $2S^{2-}/S_2^{2-}$ dichotomy in rhomboidal M_2S_2 frameworks can be governed by the nature of the metals.[2] An actual μ-η^2-η^2 S_2^{2-} disulfide bridge (S−S = 2.25 Å) is observed in the planar complex $[L_2Cu(\mu\text{-}S_2)CuL_2]$ (L_2 = monoanionic dinitrogen chelate)[9] and must be associated to Cu(II) ions (d^9 centers, strongly antiferromagnetically coupled). Conversely, other isoelectronic species of the Ni triad must be clearly formulated as $L_2M(\mu\text{-}S)_2ML_2$ (L = uncharged $2e^-$ donor), especially in view of the large S−S separations of about 3.0 Å.[10,11] In this case, the d^8-d^8 configuration is preferred over the d^9-d^9 one, and S−S coupling is excluded. The critical role played by copper is also at the origin of a fierce debate[12] about trigonal bipyramidal $[(L_2Cu)_3S_2]^{3+}$ compounds (paramagnetic) bicapped by two sulfur atoms.[13] The argument is whether at the S−S distance of about 2.7 Å there is already an incipient S_2^{2-} unit or the two sulfidos stay uncoupled ($2Cu^{II}Cu^{I}$ vs $2Cu^{II}Cu^{III}$ configuration). Again the latter option is to be excluded for analogues of the Ni triad.[14]

Trying to define better the parameters for the S−S coupling, another CCDC analysis[4] of planar $(L_2M)_2S_2$ structures (some d^8-d^8 species have a puckered M_2S_2 framework[11]) highlighted the surprisingly different geometry of the structures of $(Ph_3P)_2Pt(\mu\text{-}S)_2Pt(PPh_3)_2$ (**1**, refcode = QINYUH[15]) and $(Ph_2PyP)_2Pt(\mu\text{-}S)_2Pt(PPh_2Py)_2$ (**2**, YIJNEK[10]). From the chemical and steric viewpoints, the two compounds are almost identical having a single pyridyl substituent in place of a phenyl one at each phosphine ligand. Therefore, the different S−S distance (2.69 vs 3.01 Å, in **1** and **2**, respectively) appears most surprising (see Scheme 2). Even more perplexing is the fact that, while the Pt−S distances in **2** are typical of these bonds (>2.3 Å), **1** features *the shortest distance* ever reported (2.068 Å), and the other independent one is not much longer (2.110 Å). The Pt_2S_2 rhombuses are similar (both diagonals are equally elongated by 0.2 Å in **2**) but some puckering at the S−S vectors is observed only for **1** (about 168°).

The complex $[(Ph_3P)_2Pt(\mu\text{-}S)_2Pt(PPh_3)_2]^{2+}$ is known since 1971[16] and has received much attention from the chemical viewpoint[17] It is prone to react with electrophiles at the sulfur bridge(s)[18] but it is also stabilized by hydrogen bonding ($S\cdots HOCH_2CH_3$) as recently shown by the structure of its adduct with ethanol.[19] Remarkably, the Pt−S bonds in the structure of the adduct are almost 0.3 Å longer than in **1**,[15] hence close to those in **2**.[10] Such a dramatic effect of the hydrogen bonding over the first coordination sphere of the metals is hardly plausible.

By deeming as impossible any disulfide coupling in Pt_2S_2 frameworks, this paper illustrates all the evidence that allowed us reformulating the skeletal nature of **1**, including a new preparation and crystal analysis of another platinum dimeric complex that does not contain sulfur.

Discussion

Theoretical Underpinnings of the Variable Distance between Sulfur Bridges. By looking at the histogram of Figure 1a, among the 4200 observed Pt−S bonds of any type (average value = 2.318 Å), those in **1** (QINYUH, in the histogram at the left side) are evident outliers. Figure 1b is relative to the distribution of S−S distances in 557 samples of planar or quasi-planar M_2S_2 frameworks. The highest frequency of values is near 3.6 Å, that is, almost the sum of two sulfido radii (1.84 Å). There are also S−S distances <2.3 Å, which imply an actual disulfido bridge. As suggested elsewhere,[2a,12] the scattered values around 2.7−2.9 Å suggest possible S···S coupling in some case, and **1** clearly falls in this zone.

The qualitative theoretical underpinnings of the $2S^{2-}/S_2^{2-}$ dichotomy are conveniently outlined in Scheme 3, which shows the specific MO underlying one of the four M−S bonds in M_2S_2 frameworks. The strength of the interaction between the *in-phase* combination of d_π metal orbitals and the S−S σ^* antibonding level depends on the metal orbital energy and the S−S distance. When this is large (say over 3.0 Å), σ^* lies low in energy (black bar at the right side), so that two sulfido groups host the bonding electrons and act as donors toward the empty combination of d_π metal hybrids (typical picture of the d^8-d^8 configuration). Already at this

(9) (a) Brown, E. C.; Aboelella, N. E.; Reynolds, A. M.; Aullòn, G.; Alvarez, S.; Tolman, W. B. *Inorg. Chem.* **2004**, *43*, 3335. (b) Aullòn, G.; Alvarez, S. *Eur. J. Inorg. Chem.* **2004**, 4430–4438.
(10) Yam, V. W.-W.; Yeung, P. K.-Y.; Cheung, K.-K. *J. Chem. Soc., Chem. Commun.* **1995**, 267–269.
(11) (a) Novio, F.; Mas-Balleste, R.; Gallardo, I.; Gonzalez-Duarte, P.; Lledos, A.; Vila, N. *Dalton Trans.* **2005**, 2742. (b) Vicic, D. A.; Jones, W. D. *J. Am. Chem. Soc.* **1999**, *121*, 4070. (c) Capdevila, M.; Carrasco, Y.; Lledos, A.; Sola, J.; Ujaque, G.; Clegg, W.; Coxall, R. A.; Gonzalez-Duarte, P. *Chem. Commun.* **1998**, 597.
(12) Alvarez, S.; Hoffmann, R.; Mealli, C. A debate paper submitted for publication, 2008.
(13) (a) Brown, E. C.; York, J. T.; Antholine, W. E.; Ruiz, E.; Alvarez, S.; Tolman, W. B. *J. Am. Chem. Soc.* **2005**, *127*, 13752. (b) York, J. T.; Bar-Nahum, I.; Tolman, W. B. *Inorg. Chem.* **2007**, *46*, 8105.
(14) Examples of $[L_6Ni_3S_2]^{2+}$ species have S-S distances in the range 2.67−2.95 Å. (a) Cecconi, F.; Ghilardi, C. A.; Midollini, S.; Orlandini, A. *Z. Naturforsch. B* **1991**, *46*, 1161. (b) Cecconi, F.; Ghilardi, C. A.; Midollini, S.; Orlandini, A.; Vacca, A.; Ramírez, J. A. *J. Chem. Soc., Dalton Trans.* **1990**, 773. (c) Fenske, D.; Fleischer, H.; Krautscheid, H. *Z. Naturforsch. B* **1990**, *45*, 127. (d) Ghilardi, C. A.; Midollini, S.; Orlandini, A.; Scapacci, G. *J. Chem. Soc., Dalton Trans.* **1992**, 2909. (e) Haiduc, I.; Semeniuc, R. F.; Campian, M.; Kravtsov, V. C.; Simonov, Y. A. *Polyhedron* **2003**, *22*, 2895. (f) Matsumoto, K.; Saiga, N.; Tanaka, S.; Ooi, S. *J. Chem. Soc., Dalton Trans.* **1991**, 1265. (g) Vicic, D. A.; Jones, W. D. *J. Am. Chem. Soc.* **1999**, *121*, 7606.
(15) Li, H.; Carpenter, G. B.; Sweigart, D. A. *Organometallics* **2000**, *19*, 1823–1825.
(16) Ugo, R.; La Monica, G.; Cenini, S.; Segre, A.; Conti, F. *J. Chem. Soc. A,* **1971**, 522.
(17) Audi Fong, S.-W.; Andy Hor, T. S. *J. Chem. Soc., Dalton Trans.* **1999**, 639–651.
(18) (a) Mas-Ballesté, R.; Aullón, G.; Champkin, P. A.; Clegg, W.; Mégret, C.; González-Duarte, P.; Lledós, A. *Chem.—Eur. J.* **2003**, *9*, 5023. (b) Aullón, G.; Capdevila, M.; Clegg, W.; González-Duarte, P.; Lledós, A.; Mas-Ballesté, R. *Angew. Chem., Int. Ed.* **2002**, *41*, 2776. (c) González-Duarte, P.; Lledós, A.; Mas-Ballesté, R. *Eur. J. Inorg. Chem.* **2004**, 3585.
(19) Henderson, W.; Thwaite, S.; Nicholson, B. K.; Andy Hor, T. S. *Eur. J. Inorg. Chem.* **2008**, 5119–5124.

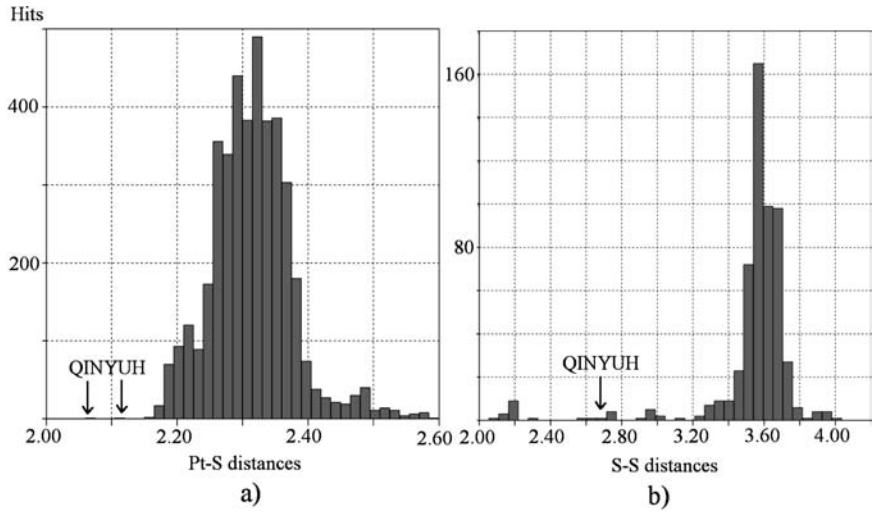

Figure 1. (a) Histogram for the distribution of all Pt−S distances (4189 cases) found for platinum metal complexes. (b) Histogram for the distribution of S−S distances in 557 cases of planar M_2S_2 frameworks (torsion angle at the S−S vector between 160° and 200°).

Scheme 3

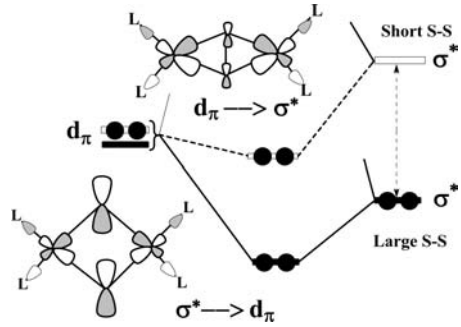

point, the small donation triggers some partial depopulation of σ^*, hence an incipient S−S coupling. The effect is synergic since the shorter is S−S, the nearer lies σ^* to d_π and the larger is the donation.

The energy of d_π depends on parameters such as the nature of the metals, the strength of the terminal ligands as donors, and the opening of the L−M−L angle.[12] Importantly, there is a correlation between M−S and S−S bonds. At some point, the S−S σ^* level can be higher in energy than the d_π one (as indicated by the blank bars in Scheme 3) and formally metal back-donation replaces the donation from the sulfido ions. This also requires a change of the metal oxidation state. If the S−S bond is strong, the σ^* level lies so high in energy that the interaction with the d_π metal levels is very small.[12] This is the case of the aforementioned d^9-d^9 system $L_2Cu(\mu\text{-}S_2)CuL_2$,[9] in which σ^* is only 8% occupied (result from EHMO calculations[20]). In contrast, the σ^* population is as large as 75% in a Pt_2S_2 model of **2**,[10] where S−S is about 3.01 Å. Shortening of the latter value by 0.32 Å (as in **1**) maintains the σ^* population relatively high (67%) and the actual S−S coupling is still improbable. In comparison, at the same S−S distance of 2.7 Å, the σ^* population is halved[2,12] in the TBP copper complex $[(L_2Cu)_3S_2]^{3+}$ (L_2 = dinitrogen ligand)[13a] for which an elongated disulfide unit has been invoked.[2,12]

Although apparently dichotomous, the Pt_2S_2 framework, suggested by the structures of **1** and **2**, cannot be affected by different sterical problems, but also the electronic ones seem improbable. Conversely recall that for copper, the dichotomy of Cu_2O_2 planar cores, stabilized by either a short or a long O−O separation, has been instead shown, experimentally.[21] To check further the different behavior of platinum, we performed density functional theory (DFT) optimizations[22] of the simplest model $(H_3P_3)_2Pt(\mu\text{-}S)_2\text{-}Pt(PH_3)_2$ with the Pt_2S_2 cores of both **1** and **2**. Convergence was invariably reached at the S···S distance of 3.1 Å, that is, slightly larger than in **2**. Single point calculations with all phenyl substituents showed a huge destabilization energy (~467 Kcal mol^{-1}) for the geometry of **1** versus **2**. This clearly indicates that the sulfido σ lone pairs are definitely repulsive to each other, if there is no good way of transferring electrons to the metals.

Questionable Crystallographic Features of the Compounds $(Ph_3P)_2Pt(\mu\text{-}S)_2Pt(PPh_3)_2$, 1, and $[(Ph_3P)_2Pt(\mu\text{-}OH)_2\text{-}Pt(PPh_3)_2](BF_4)_2$, 3. Eventually, we started wondering whether the structure **1** could have been incorrectly formulated. A similar doubt was raised by other authors, who attributed the incongruent geometry to a possible oxidation of the compound during crystallization.[23] Further suspicions came from a careful reading of the original structural report and CIF file for **1**.[15] The authors state that crystals were found only after their target compound $[(CO)_2Mn(\mu_2\text{-}\eta^6\text{-}2\text{-}(C_6H_4CH{=}C(S)CH_3)Pt(PPh_3)_2]BF_4$ sat for 2 months in a solution containing CH_2Cl_2 and Et_2O. While the main product was fully characterized, only an X-ray analysis could be carried out for **1**, which was considered a subproduct and

(20) Calculations performed with the CACAO package. (a) Mealli, C.; Proserpio, D. M. *J. Chem. Educ.* **1990**, *67*, 399. (b) Mealli, C.; Ienco, A.; Proserpio, D. M. *Book of Abstracts of the XXXIII ICCC*; ICCC: Florence, Italy, 1998; p 510.

(21) (a) Tolman, W. B. *Acc. Chem. Res.* **1997**, *30*, 227–237. (b) Lewis, E. A.; Tolman, W. B. *Chem. Rev.* **2004**, *104*, 1047–1076. (c) Brown, E. C.; Aboelella, N. W.; Reynolds, A. M.; Aullòn, G.; Alvarez, S.; Tolman, W. B. *Inorg. Chem.* **2004**, *43*, 3335–3337.

(22) Frisch M. J.; et al. *Gaussian 03*, Revision C.02; Gaussian Inc.: Wallingford, CT, 2004.

(23) Aullon, G.; Hamidi, M.; Lledos, A.; Alvarez, S. *Inorg. Chem.* **2004**, *43*, 3702–3714.

Table 1. Original Direct and Reciprocal Cell Parameters Reported for **1** and **3**, As Well As Those of the Newly Prepared Crystals of $[(Ph_3P)_2Pt(\mu\text{-}OH)_2Pt(PPh_3)_2](BF_4)_2$

crystal data	compound **1**, *QINYUH*	compound **3**, *ZOTLAV*	newly prepared $[(Ph_3P)_2Pt(\mu\text{-}OH)_2Pt(PPh_3)_2](BF_4)_2$
crystal system	monoclinic	monoclinic	monoclinic
chemical formula	$C_{72}H_{60}P_4Pt_2S_2 \cdot 2C_6$[a]	$C_{72}H_{62}P_4Pt_2O_2\ 2BF_4$	$C_{72}H_{62}P_4Pt_2O_2\ 2BF_4$
space group	$C_{2/c}$	$C_{2/m}$	$C_{2/c}$
a, Å	17.2348(13)	17.183(5)	17.168(3)
b, Å	18.2934(15)	18.243(4)	18.242(5)
c, Å	20.4947(16)	13.539(4)	20.545(3)
β, deg	91.325(3)	130.66(2)	91.563(13)
V (direct cell), Å^3	6459.9(9)	3219(2)	6432(2)
*a**, Å^{-1}	0.058037	0.075724	0.058270
*b**, Å^{-1}	0.054666	0.054597	0.054819
*c**, Å^{-1}	0.048806	0.098477	0.048692
*β**, deg	88.675	49.34	88.43
*V** (recipr. cell), Å^{-3}	0.000155	0.000310	0.000155
Z[b]	4	2	4
Z′[c]	0.5	0.25	0.5

[a] Unidentified solvent molecule. [b] Number of molecules in the unit cell. [c] Number of molecules in the asymmetric unit.

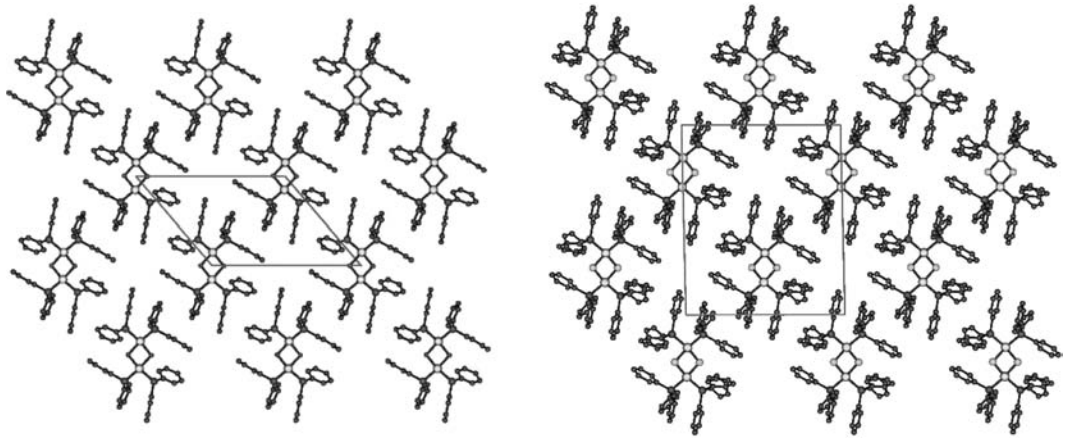

Figure 2. Packing diagrams showing the bimetallic units in **1** and **3** (left and right, respectively) projected down their equal *b* axis. In **1** (space group $C_{2/c}$), the complex lies approximately on the 0, 1/4, 0 plane, while in **3** (space group $C_{2/m}$), the plane containing the metals is 0, 0, 0.

presented in the paper as a footnote.[15] We started wondering whether a serendipitous reaction with oxygen (from either the atmosphere or another source) could have occurred. The hypothesis of lighter bridging atoms was prompted by the sulfur thermal ellipsoids, which are large (U_{eq}=0.154(2) Å^2) especially in comparison with those of the Pt and P atoms (U_{eq} = 0.039 and 0.044 Å^2, respectively).

The Cambridge database[4] provides about 1280 hits of Pt−O bonds of all types with an average distance of 2.055 Å but no example of $Pt_2(\mu\text{-oxo})_2$ frameworks. In contrast, there are about 50 $Pt_2(\mu\text{-hydroxo})_2$ structures with an average Pt−O distance of just 2.068 Å. These bridges imply the presence of two anions, which were not formulated for **1** although unidentified solvent molecules were indicated. On the other hand, tetrafluoborate anions must have been present in solution, as they are part of the reaction's main product.[15] In short, we postulated that **1** could be the species $[(Ph_3P)_2Pt(\mu\text{-}OH)_2Pt(PPh_3)_2](BF_4)_2$, **3**, whose structure is also present in the literature (refcode = ZOTLAV).[24] The identity of **1** and **3** could be easily validated, provided that the crystals had the same cell. However, as shown in Table 1, the comparison is not conclusive. The parameters *a* and *b* are equal but *c* and *β* are different. Moreover, the volume of the cell **1** is precisely double, as is the ratio between the Z values. Also, the space groups are different, namely $C_{2/c}$ and $C_{2/m}$ for **1** and **3**, respectively. This means that the dinuclear unit in **1** has only an inner 2-fold axis, while in **3** it contains also a perpendicular mirror plane (centrosymmetric molecule).

This difference is appreciated from the packing diagrams of Figure 2, both projected down the common *b* axis with the other equal axis *a* being horizontal.

The right side picture clearly shows that the $P_4Pt_2O_2$ plane in **3** (coinciding with *ac*) splits in two parts each phosphine ligand and one phenyl ring, in particular. Nonetheless, the in plane oxygen bridges of **3** have thermal ellipsoids that are anomalously elongated along the *b* axis (U_{22} = 0.35 Å^2), and a possible break of the mirror symmetry is suggested. In contrast, the $C_{2/c}$ space group of **1** has no mirror symmetry, since the main plane *ac* is a glide plane, with respect to which the bimetallic skeleton is shifted by 1/4 along *b*.

Besides the questionable assignment of the bridging atoms in **1**, the structure of **3** may have been solved with an ill-defined crystalline cell. By looking at the cell metrics, it has not been difficult to construct the matrices **I** and **II**, which interconvert direct and reciprocal cells. According to matrix **I**, the *c* axis of **1** matches the vector sum between the *a* and doubled *c* axes of **3**. This also explains why also the ratio between the cell volumes is 2:1.

(24) Li, J. J.; Li, W.; Sharp, P. R. *Inorg. Chem.* **1996**, *35*, 604–613.

$$\begin{pmatrix} 1 & 0 & 0 \\ 0 & 1 & 0 \\ 1 & 0 & 2 \end{pmatrix} \quad (1)$$

$$\begin{pmatrix} 1 & 0 & -0.5 \\ 0 & 1 & 0 \\ 0 & 0 & 0.5 \end{pmatrix} \quad (2)$$

Consequently, the reported structural solution and refinement of **3** appears questionable because it was determined by using only one-half of the possible reflections (see below). Conversely (and likely thanks to the usage of an area detector diffractometer), the data set collected for **1** seems to be complete. To clarify this point, Figure 3 shows how matrix **II** (inverse and transpose of **I**) correlates the reciprocal axes in the *h0l* section of the lattice. The new a^*_n axis is obtained by combining the original a^*_o and halved c^*_o (negative) axes. Sample reflections are expressed in terms of both the original (a^*_o, c^*_o) and transformed (a^*_n, c^*_n) axes. With the former choice, all the reflections having indexes $h + l = 2n + 1$ (gray circles) were neglected, and this is true for any k value.

Since none of the original data sets for **1** and **3** was available to us, we decided to repeat the experimental synthesis and X-ray structure determination of **3**. The compound $[(Ph_3P)_2Pt(\mu\text{-}OH)_2Pt(PPh_3)_2](BF_4)_2$ was obtained from an aqueous solution. A preliminary cell determination, using a diffractometer with a point detector[25] and in the absence of fine peak-searching techniques, initially seemed to confirm the cell published for **3**, but an area detector (see the Experimental Section) clearly revealed the identity with the cell of **1**, hence the space group $C_{2/c}$. The reflections were measured up to $\vartheta = 25.49°$ and the *hkl* ones with $h + l = 2n + 1$ are generally weak but not negligible. In fact, 1062 (over a total of 5892) were considered as observed ($I > 2\sigma(I)$), with an average intensity of 3840 counts The reflections with $h + l = 2n$ are double in number (2224) and, on the average, they are about four times more intense than those of the previous group. The weaker reflections seem attributable to the peculiar arrangement of the heavier dinuclear units (Pt and P atoms), which are all parallel to each other (see Figure 2). The scarce off-plane electron density (mainly that originating the systematically weak reflections) is largely due to interspersed light atoms of the phenyl rings and BF_4^- anions.

Structure of $[(Ph_3P)_2Pt(\mu\text{-}OH)_2Pt(PPh_3)_2](BF_4)_2$ at Different Temperatures and DFT Modeling. Figure 4 shows an Oak Ridge Thermal Ellipsoid Plot (ORTEP) drawing[26] of the newly determined dication $[(Ph_3P)_2Pt(\mu\text{-}OH)_2Pt(PPh_3)_2]^{2+}$ (H atoms not shown) at room temperature. Two BF_4^- anions (on 2-fold axes) are affected by usual disorder. Geometric data appear in the first column of Table 2.

The Pt-bridge bonds are somewhat asymmetric (2.088(5) and 2.128(5) Å), but the distances are consistent with oxygen bridges. The complex dication is not centrosymmetric as it was in the original structure of **3**.[24] The puckering, already observed for **1**, is confirmed by the 167.3(5)° torsion at the O···O vector. This feature is typical for $Pt_2(\mu\text{-}OH)_2$ frameworks and the dihedral angle being most pronounced in $[\{(Ph_2PCH_2CH_2CH_2PPh_2)Pt\}_2(\mu\text{-}OH)_2]^{2+}$ (147°).[27]

The present structure refines to a somewhat lower R value than the original one[24] (0.0497 vs 0.059). The oxygen thermal ellipsoids are about one-fourth smaller than before along the b axis (U_{22} = 0.089(5) Å^2). While this value may be acceptable for routine crystallographic work, here it is an indication of some persisting disorder. Attempts of refining alternative oxygen positions (by using partial population parameters) were unsuccessful, also because in the ΔF syntheses the atomic images appear elongated but never split.

The possible origin of the disorder is suggested by DFT optimizations of the simple model $[(H_3P)_2Pt(\mu\text{-}OH)_2Pt(PH_3)_2]^{2+}$ (see Figure 5). Two minima, **3a** and **3b**, were optimized with bent (154.5°) and planar Pt_2O_2 skeletons,

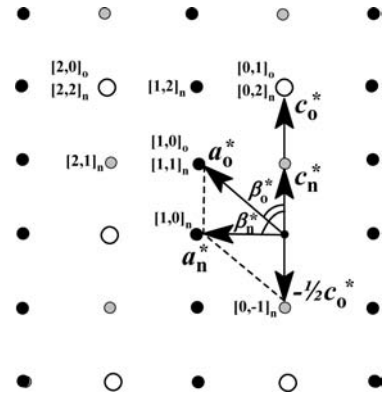

Figure 3. Reciprocal cell plane perpendicular to the unique b^* axis (k = 0). The new axes (a^*_n and c^*_n) are obtained by applying matrix **II** to the original cell of **3** (a^*_o and c^*_o). Black circles refer to reflections extinct by C-centring ($h + k = 2n + 1$); the gray ones were not collected in the original structure determination of **3** (*hkl* with $h + l = 2n + 1$). Some examples illustrate the relation between original $[h0l]_o$ and new $[h0l]_n$ reflection indexes.

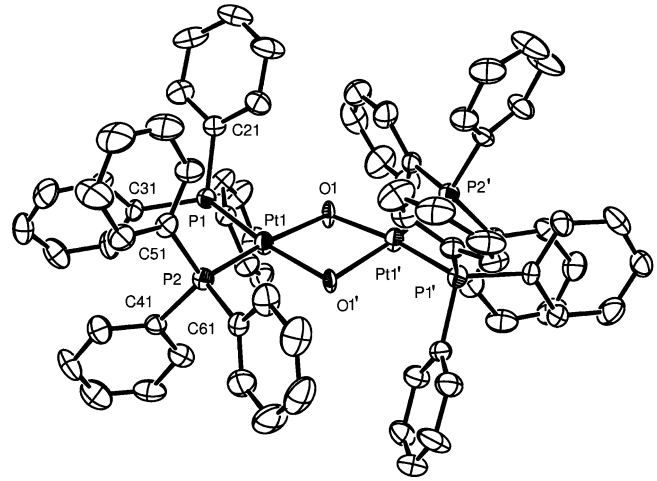

Figure 4. View of the complex dication $[(Ph_3P)_2Pt(\mu\text{-}OH)_2Pt(PPh_3)_2]^{2+}$ (omitted H atoms), as obtained from RT data (the primed atoms related by the symmetry transformation $-x$, y, $-z + 1/2$ in the space group $C_{2/c}$).

(25) The diffractometer with a punctual detector was a Philips PW 1100, whereas the machine equipped with an area detector was an Oxford Diffraction Xcalibur3 (see ExpErimental Section).

(26) Burnett, M. N.; Johnson, C. K. *ORTEP-III*; Oak Ridge National Laboratory: Oak Ridge, TN, 1996.

(27) Bandini, A. L.; Banditelli, G.; Demartin, F.; Manassero, M.; Minghetti, G. *Gazz. Chim. Ital.* **1993**, *123*, 417.

Table 2. Comparison of Selected Geometric Parameters (Å or deg) for the Dication $[(Ph_3P)_2Pt(\mu\text{-}OH)_2Pt(PPh_3)_2]^{2+}$ in the Present and the Original Work of Reference 24

	RT	150 K molecule 1	150 K molecule 2	ZOTLAV (ref 24)
Pt(1)−O(1)	2.128(5)	2.144(5)	2.155(6)	2.072[11]
Pt(1)−O(1)′	2.088(5)	2.045(5)	2.047(6)	2.053[11]
Pt(1)−P(1)	2.237(2)	2.260(3)	2.250(2)	2.234[4]
Pt(1)−P(2)	2.217(2)	2.213(3)	2.201(2)	2.206[4]
Pt(1)−Pt(1)′	3.1793(8)	3.1318(10)	3.1969(10)	3.153[2]
O(1)−Pt(1)−O(1)′	81.27(19)	81.8(2)c	80.5(3)	80.3[4]
P(1)−Pt(1)−P(2)	98.76(8)	98.62(10)	98.42(9)	99.08[14]
O(1)−Pt(1)−P(1)	88.80(14)	87.97(17)	88.77(18)	88.8[3]
O(1)−Pt(1)−P(2)	172.40(13)	172.79(15)	172.78(18)	172.1[3]
O(1)′−Pt(1)−P(1)	170.07(14)	169.51(17	168.85(19)	169.1[3]
O(1)′−Pt(1)−P(2)	91.17(15)	91.52(18)	92.26(19)	91.8[3]
Pt(1)−O(1)−O(1)′−Pt(1)′	167.3(5)	162.7(4)	170.9(5)	180.0

respectively. In **3a**, the OH bonds are equally oriented with respect to the Pt_2O_2 core but point to opposite directions in **3b**. Since **3a** is more stable by only 1.5 kcal mol^{-1} both conformations likely coexist in the crystal (probably the bulky phenyl substituents are not so influential). Moreover, the Transition State (**3c**) for the interconversion between two equivalent puckered models lies only 3.5 kcal mol^{-1} above **3a**. Notice that **3c**, with one OH vector in the corresponding Pt_2O plane, indifferently leads to a puckered or planar structure.

According to the computational indications, the geometries can easily interconvert at room temperature, hence cause a dynamical disorder in the crystal. Assuming that, at 150 K, only one conformation is frozen, a new data collection was carried out at this temperature. An evident phase transition must have occurred since the cell is no more C-centered (the *hkl* reflections are present for $h + k = 2n + 1$). The new space group $P_{2/n}$ implies a double number of independent variables to be refined, that is, two independent dimers, which differ in particular (see Table 2) for the amount of puckering at the O−O′ vector (PtOOPt dihedral angle, 170.9° vs. 162.7°).

As visually shown in Figure 6 by the projection of the $P_{2/n}$ cell down the *a* axis (*b* horizontal), the unique RT dimer now adopts more puckered (at $b = 1/2$) and more planar (at $b = 0$) structures.

Unfortunately, the oxygen disorder is not fully solved, as shown by the persistently high U_{22} components of the thermal ellipsoid (0.087 and 0.073 $Å^2$, at 150 K vs the 0.089 $Å^2$ value 293 K). Although the final ΔF syntheses for the 150 K structure show some split images of the oxygen bridges, the refinement of partial population parameters was not deemed satisfactory. Perhaps, an useful strategy to prevent disorder could be a crystallization of the sample at the same low temperature of data collection (150 K), but this seems unfeasible for the aqueous chemistry of the system. Eventually, any further experimental attempt was dismissed, also in view of the significant indications already attained. In view of the small conformational barrier, the disorder has a dynamic nature at RT, whereas by lowering the temperature, the molecules can be in principle frozen but differently puckered molecules may overlap and give rise to statistical disorder.

Final Remarks

As stated by Hoffmann,[28] chemistry is interpretable, not only through reductivism (i.e., the usage of higher level physical and mathematical laws, including those of quantum mechanics) but also from the horizontal comparison of homogeneous cases. Structural correlations highlight chemical bonding and functionality. In our experience, a combination of the latter approach with a computational strategy was fruitful, but sometimes we had to revise an apparently good theoretical model because of its inconsistency with the experimental data. Sometimes, the inconsistencies found in series of structures were due to the poor determination of

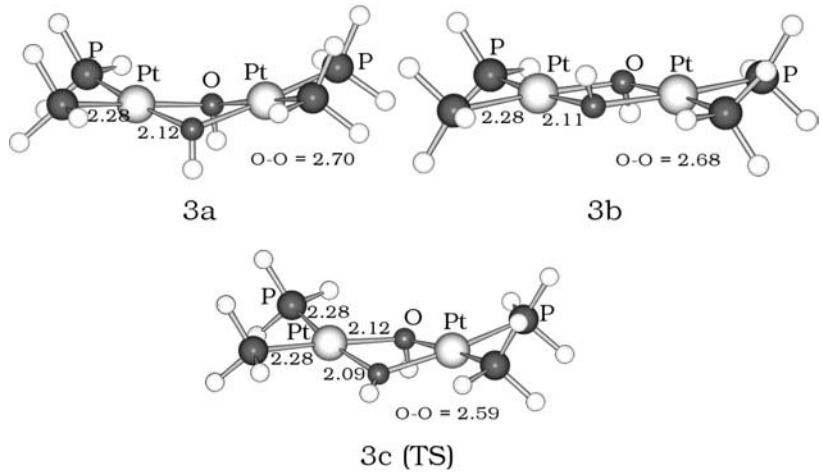

Figure 5. Optimized models $[(H_3P)_2Pt(\mu\text{-}OH)_2Pt(PH_3)_2]^{2+}$ with puckered (**3a**) and planar (**3b**) Pt_2O_2 cores. The model **3c** is the transition state (TS) between two mirrored puckered structures of the type **3a**.

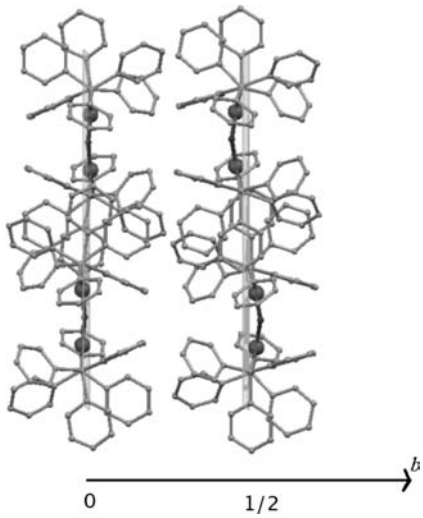

Figure 6. Projection of the $P_{2/n}$ cell down the *a* axis (*b* horizontal). At 150 K, quasi-planar and puckered $[(Ph_3P)_2Pt(\mu\text{-}OH)_2Pt(PPh_3)_2]^{2+}$ dimeric cations become distinguishable.

the hydrogen atoms from X-ray data. For instance, in a systematic study[29] to define the limits of *agostic* interactions[30] (namely, the M-η^2-C-H vs M-$\eta^3$$CH_2$ coordination), a correlation was found between the bonding mode and the length of the chain that connects the metal to the dangling CH_3 group. Some evident outlier was associated to the poor localization of the CH_3 hydrogen atoms from X-ray rather than neutron diffraction data.

The S−S and Pt−S short distances in one Pt_2S_2 compound **1** were puzzling because they were clearly inconsistent with the wider chemical knowledge on bonding and theoretical arguments.[2,12] The picture seemed particularly mystifying because S atoms are usually well characterized by X-ray diffraction experiments. On the other hand, we were aware of examples showing how chemical/theoretical considerations can occasionally lead to a different interpretation of a crystalline structure.[31] The new structure determination of $[(Ph_3P)_2Pt(\mu\text{-}OH)_2Pt(PPh_3)_2](BF_4)_2$ (**3**) undoubtedly proved that this is also the correct formulation of the compound reported as $(Ph_3P)_2Pt(\mu\text{-}S)_2Pt(PPh_3)_2$ (**1**).[10] Therefore, any other conjecture, concerning either a chemical change during the crystallization of **1**[23] or other implications for the S−S coupling and the record shortest Pt−S distance, has to be dismissed.

A rare case cannot question the reliability of single crystal X-ray diffraction experiments as the safest and most accurate method for observing matter at the atomic level. Only exceptionally, it might be useful to reconsider with criticism a crystal structure before dismissing an apparently rational chemical or theoretical model.

Experimental Section

Synthesis of the Complex $[(Ph_3P)_2Pt(\mu\text{-}OH)_2Pt(PPh_3)_2](BF_4)_2$. The synthesis of compound **3**,[24] attempted according to a literature method,[32] leads to a mixture of different products. Thus, we followed an alternative procedure already adopted for analogous derivatives with the $PMePh_2$ ligand.[33] The starting materials, NaOH, $AgBF_4$, and *cis*-$(PPh_3)_2PtCl_2$, were reagent grade, the last obtained according to a known method.[34] All manipulations were performed under air. A solution, prepared by dissolving 194.7 mg of $AgBF_4$ in a mixture of 3 mL of EtOH and 0.4 mL of H_2O, was added dropwise to the solution of the platinum complex (i.e., 395 mg dissolved in 13 mL of dichloromethane) under a vigorous stirring. AgCl was filtered off, and then 5 mL of an aqueous solution of NaOH 0.1 N were added. After stirring for 10 min, the solvent was partially evaporated under vacuum. The white precipitate was recovered by filtration under air, washed twice with water (2 × 4 mL), and dried under vacuum. The crude product **3** was recrystallized from CH_2Cl_2/Et_2O, the yield of pure product being 576 mg (70%). Suitable crystals for X-ray diffraction were obtained by slow diffusion of ethyl ether into a saturated solution of the complex in dichloromethane.

Elemental analysis (%) calcd for $C_{72}H_{62}O_2P_4B_2F_8Pt_2$(1646.92): C 52.51, H 3.79; found: C 52.48, H 3.70. The $^{31}P\{^1H\}$ and ^1H NMR spectra were recorded on Bruker Avance DRX-400 and compare well with those of the NO_3 analogue.[35] ^1H NMR (DMSO-d_6, 20 °C, 200.13 MHz, TMS reference): δ = 7.2−7.5 [m, 60 H, Ph], 3.4 [s broad, 2 H, OH];$^{31}P\{^1H\}$ NMR (DMSO-d_6, 20 °C, 81.01 MHz, 85% H_3PO_4 reference): δ = 6.5 (s, $^1J_{PPt}$ = 3732.6 Hz) ppm.

Structure Determination of $[(Ph_3P)_2Pt(\mu\text{-}OH)_2Pt(PPh_3)_2](BF_4)_2$. The crystal data of compound **3**, collected at room temperature (RT) and at 150 K, are presented in Table 3. The X-ray experiments were carried out on a CCD diffractometer with Mo Kα radiation. The program CrysAlis CCD[36] was used. Data reductions (including absorption corrections) were carried out with the program CrysAlis RED.[37] The RT atomic coordinates, obtained by the direct methods in Sir97,[38] are consistent with those originally reported for structure **3**[24] after applying the transformation matrix **I**. Structure refinements were performed with SHELXL[39] using the full-matrix least-squares method for all the available F^2 data. All the non-hydrogen atoms were refined anisotropically, except for those of the disordered BF_4^- anions (at the low temperature this was necessary only for one of the four anions). Restraints were used on the B−F distances only for the RT data set. The H atoms were fixed in calculated positions and refined isotropically with thermal factors 20% larger than the atom to which they are bound. The hydrogen atoms of the OH bridges were not included. All calculations were performed under

(28) Hoffmann, R. *THEOCHEM* **1998**, *424*, 1–6.
(29) Baratta, W.; Mealli, C.; Herdtweck, E.; Ienco, A.; Mason, S. A.; Rigo, P. *J. Am. Chem. Soc.* **2004**, *126*, 5549–5562.
(30) (a) Brookhart, M.; Green, M. L. H.; Wong, L.-L. *Prog. Inorg. Chem.* **1988**, *36*, 1. (b) Crabtree, R. H.; Hamilton, D. G. *Adv. Organomet. Chem.* **1988**, *28*, 299. (c) Crabtree, R. H. *Angew. Chem., Int. Ed. Engl.* **1993**, *32*, 789. (d) Yao, W.; Eisenstein, O.; Crabtree, R. H. *Inorg. Chim. Acta* **1997**, *254*, 105. (e) Ogasawara, M.; Saburi, M. *Organometallics* **1994**, *13*, 1911.
(31) As possible examples, see: (a) von Schnering, A. G.; Vu, D. *Angew. Chem., Int. Ed. Engl.* **1983**, *22*, 408. (b) Müller, T. *Angew. Chem., Int. Ed.* **2002**, *41*, 2276. (c) Flower, K. R.; Pritchard, R. G.; McGown, A. T.; Müller, T. *Angew. Chem., Int. Ed.* **2006**, *45*, 6535.
(32) Bushnell, G. W.; Dixon, K. R.; Hunter, R. G.; McFarland, J. J. *Can. J. Chem.* **1972**, *50*, 3694–3699.
(33) Longato, B.; Bandoli, G.; Dolmella, A. *Eur. J. Inorg. Chem.* **2004**, 1092–1099.
(34) Bailar, J. C., Jr.; Itatani, H. *J. Chem. Soc.* **1969**, 1618–1620.
(35) Longato, B.; Montagner, D.; Bandoli, G.; Zangrando, E. *Inorg. Chem.* **2006**, *45*, 1805–1814.
(36) *CrysAlisCCD*, Version 1.171.31.2 (release 07-07-2006 CrysAlis171.NET); Oxford Diffraction Ltd.: Oxfordshire, U.K., 2006.
(37) *CrysAlis RED*, Version 1.171.31.2 (release 07-07-2006 CrysAlis171.NET); Oxford Diffraction Ltd.: Oxfordshire, U.K., 2006.
(38) Altomare, A.; Burla, M. C.; Camalli, M.; Cascarano, G. L.; Giacovazzo, C.; Guagliardi, A.; Moliterni, A. G. C.; Polidori, G.; Spagna, R. *J. Appl. Crystallogr.* **1999**, *32*, 115–119.
(39) Sheldrick, G. M. *Acta Crystallogr.* **2008**, *A64*, 112–122.

Table 3. Crystal Data for $[(Ph_3P)_2Pt(\mu\text{-}OH)_2Pt(PPh_3)_2](BF_4)_2$ at Different Temperatures

empirical formula	$C_{72}H_{62}B_2F_8O_2P_4Pt_2$	$C_{72}H_{62}B_2F_8O_2P_4Pt_2$
formula weight	1646.90	1646.90
temperature (K)	293(2)	150(2)
wavelength (Å)	0.71069	0.71069
crystal system	monoclinic	monoclinic
space group	$C_{2/c}$	$P_{2/n}$
unit cell dimensions		
a (Å)	17.168(3)	17.061(5)
b (Å)	18.242(5)	18.278(5)
c (Å)	20.545(3)	20.443(4)
β (deg)	91.563(13)	90.890(18)
volume (Å^3)	6432(2)	6334.7(3)
Z (number of molecule in the cell)	4	4
Z' (number of molecules in the asymmetric unit)	0.5	1
calcd density (g/cm^3)	1.701	1.716
absorption coefficient (mm^{-1})	4.515	4.556
F(000)	3232	3232
crystal size (mm^3)	0.24 × 0.18 × 0.11	0.26 × 0.18 × 0.11
theta range for data collection (deg)	3.68 to 25.49.	3.75 to 32.61
limiting indexes	$-20 \le h \le 20$	$-24 \le h \le 21$
	$-22 \le k \le 21$	$-27 \le k \le 14$
	$-24 \le l \le 21$	$-29 \le l \le 30$
reflections collected	18659	47579
independent reflections	5892 [$R_{(int)} = 0.1000$]	19426 [$R_{(int)} = 0.0616$]
completeness to theta = 25.00°	98.7%	98.7%
absorption correction	multiscan	multiscan
refinement method	full-matrix LS on F^2	full-matrix LS on F^2
data/restraints/parameters	5892/6/385	19426/0/804
goodness-of-fit on F^2	0.911	1.067
final R indices [$I > 2$sigma(I)]	$R_1 = 0.0497$, $wR_2 = 0.0974$	$R_1 = 0.0841$, $wR_2 = 0.1393$
R indices (all data)	$R_1 = 0.1155$, $wR_2 = 0.1095$	$R_1 = 0.1637$, $wR_2 = 0.1578$
largest diff. peak and hole (e$^-$·Å^{-3})	1.509 and −0.985	5.128 and −2.917

the control of the WINGX package.[40] Three-dimensional drawings were made by using either ORTEP-III for Windows[26] or SCHAKAL97.[41]

DFT Calculations. Structural optimizations were carried out at the hybrid DFT level using the Gaussian03 suite of programs.[22] The method used was the Becke's three-parameter hybrid exchange-correlation functional[42] containing the nonlocal gradient correction of Lee, Yang, and Parr (B3LYP).[43] Calculations of the frequencies were performed to validate the nature of the optimized stationary points. The Stuttgart/Dresden effective core potential was used for metals.[44] The basis set used for the remaining atomic species was the 6-31G(d, p).[45]

Acknowledgment. We thank Professors Roald Hoffmann, Richard Kirchner, Stefano Midollini, and Angelo Sironi for helpful suggestions. Computing facilities have been provided by the CINECA under the agreement with CNR. This work has been performed under Progetto 7 of the Dipartimento di Progettazione Molecolare of the CNR and the FIRENZE HYDROLAB project (sponsored by Ente Cassa di Risparmio di Firenze).

Supporting Information Available: The complete ref 22 and the optimized coordinates for the species **3a**, **3b**, and **3c**. This material is available free of charge via the Internet at http://pubs.acs.org.

IC8023748

(40) Farrugia, L. J. *J. Appl. Crystallogr.* **1999**, *32*, 837–838.
(41) Keller, E. *SCHAKAL97*; University of Freiburg: Germany, 1997.
(42) Becke, A. D. *J. Chem. Phys.* **1993**, *98*, 5648.
(43) Lee, C.; Yang, W.; Parr, R. *Phys. Rev.* **1998**, *B37*, 785.
(44) Dolg, M.; Stoll, H.; Preuss, H.; Pitzer, R. M. *J. Phys. Chem.* **1993**, *97*, 5852.
(45) Hariharan, P. C.; Pople, J. A. *Theor. Chim. Acta* **1973**, *28*, 213.